CONFERENCE PRE-PRINT

CONTROL OF ENERGETIC PARTICLE MODES ON THE TCV TOKAMAK

A. JANSEN VAN VUUREN

Ecole Polytechnique Fédérale de Lausanne (EPFL), Swiss Plasma Center (SPC)

Lausanne, Switzerland

Email: anton.jansenvanvuuren@epfl.ch

J. POLEY-SANJUÁN, A. N. KARPUSHOV, M. PODESTÀ

Ecole Polytechnique Fédérale de Lausanne (EPFL), Swiss Plasma Center (SPC) Lausanne, Switzerland

S. MAZZI

IRFM-CEA Centre de Cadarache Saint Paul-lez-Durance, France

M. DREVAL

Institute of Plasma Physics, National Science Center, Kharkov Institute of Physics and Technology Kharkov, Ukraine

S. SHARAPOV

UKAEA, Culham Campus Abingdon, United Kingdom

The TCV team^a and the EUROfusion Tokamak Exploitation Team^b

^aSee the author list of B.P. Duval et al 2024 Nucl. Fusion **64** 112023.

^bSee the author list of E. Joffrin et al 2024 Nucl. Fusion **64** 112019.

Abstract

Fast-ion confinement is a key requirement for sustaining efficient plasma heating and preventing damage to plasma-facing components in future fusion reactors. Experiments on the Tokamak à Configuration Variable (TCV) have investigated energetic particle-driven instabilities and their control, focusing on Alfvén eigenmodes (AEs) and related fast-ion transport. Systematic studies using electron cyclotron resonance heating (ECRH) demonstrated robust AE suppression, with the strongest effect observed when mid-radius deposition overlapped the mode location. Suppression was reproducible regardless of whether deposition scans began on- or off-axis and applied successfully to AEs excited by both neutral beam systems. These results suggest that suppression mechanisms involve not only shear profile modifications but also changes in local density and temperature. Complementary experiments compared fast-ion behavior in negative triangularity (NT) and positive triangularity (PT) plasmas. Under MHD-quiescent conditions, confinement in NT and PT was found to be comparable and consistent with neoclassical predictions. However, NT plasmas exhibited persistent energetic geodesic acoustic modes (EGAMs), which appeared to limit TAE activity. Localized ECRH suppressed EGAMs, allowing TAEs to re-emerge, though with reduced amplitudes compared to PT. These findings confirm the potential of NT shaping as a favorable configuration for mitigating AE activity and demonstrate the role of localized heating as an effective actuator for AE control.

1. INTRODUCTION

In future fusion reactors, the confinement of energetic ions is central to sustaining plasma heating and protecting plasma-facing components [1]. Neutral beam injection and fusion-born alpha particles are expected to provide a significant fraction of plasma heating and non-inductive current drive. However, their interaction with magnetohydrodynamic (MHD) instabilities can degrade confinement and lead to enhanced losses [2]. Of particular concern are Alfvén eigenmodes (AEs), which are driven unstable by resonant interactions with suprathermal ions. Once excited, AEs can redistribute fast ions across flux surfaces, enhance losses to the wall, and reduce overall plasma performance. In addition to AEs, energetic particle-driven geodesic acoustic modes (EGAMs) and other MHD activity may further impact fast-ion transport under reactor-relevant conditions.

Mitigation and control of energetic particle instabilities are therefore essential for reliable operation of ITER and DEMO. If uncontrolled, AE-driven fast-ion transport could compromise heating efficiency, damage plasma-facing components through localized wall loading, and reduce the viability of advanced scenarios. Several control strategies have been explored in present-day devices. Resonant magnetic perturbations have been shown to modify fast-ion profiles through stochastic transport, reducing AE drive [3,4]. Localized electron cyclotron resonance heating (ECRH) and current drive (ECCD) offer another approach, altering temperature, density, and shear profiles to increase mode damping or stabilize the underlying equilibrium [5]. Plasma shaping also plays a critical role. Negative triangularity (NT) configurations, which enhance bulk confinement, have recently been identified as favorable for reducing AE activity [6,7].

The Tokamak à Configuration Variable (TCV) provides a unique platform to investigate these mechanisms. Its wide shaping flexibility [8], upgraded dual neutral beam injection system [9], and comprehensive fast-ion diagnostic suite [10] enable systematic studies of AE excitation and suppression across a range of plasma configurations. Recent experimental campaigns on TCV have focused on two complementary approaches: (i) active control of AEs through localized heating and current drive, and (ii) passive modification of AE activity through shaping, in particular NT configurations. These studies provide new insights into the physics of energetic particle instabilities and contribute directly to the control strategies required for ITER and DEMO.

2. EXPERIMENTAL SETUP

Systematic studies of AE excitation and suppression have been carried out on TCV using both co- and counter-NBI in combination with **ECRH** and ECCD. Experiments were performed in deuterium plasmas at low plasma current ($I_p \approx \pm 120 \text{ kA}$) and standard toroidal magnetic field strength $(B_{\Phi} = -1.4 \text{ T, clockwise when viewed from})$ above). For negative plasma current, NBI-1 injects co-current, while NBI-2 injects counter-current. Up to 1.7 MW of ECRH was available from launchers L1 and L4, both located at the midplane, with flexible steering allowing for radial deposition sweeps.

2.1. AE suppression by ECRH

Over recent campaigns, TCV has been used investigate beam-driven AEs [11] and their control with ECRH [12]. These studies demonstrated the potential of TCV as a testbed for energetic particle physics. However, an important limitation of early work was the reliance on off-axis NBI to

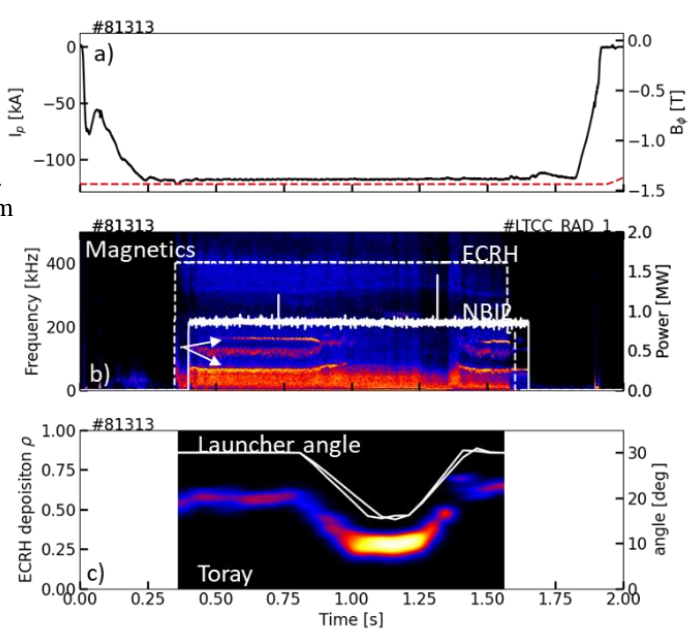


FIG 1: (a) Time trace of the plasma current (black) and toroidal magnetic field strength (red-dashed). (a) Plasma current (black) and toroidal magnetic field (red dashed). (b) Spectrogram of the magnetic pickup coils with ECRH power (dashed) and NBI-2 power (solid) overplotted. (c) TORAY-calculated ECRH power deposition versus radial position (ρ_{pol}) and time, with the two ECRH mirror angles shown as solid white lines.

drive AEs, which resulted in marginal instability and poor diagnostic coverage of the core plasma (typically

only up to $\rho \approx 0.4$). Since AE stability is sensitive to global plasma conditions, modeling of these cases was not well constrained.

To address this, a reliable on-axis scenario has been developed. Building on earlier studies, counter-NBI injection was used to reproducibly excite AEs in plasmas only slightly displaced above the midplane (z = 5 cm). More recently, scenarios with co-NBI driven AEs have also been established, enabling broader studies of control mechanisms.

2.1.1. Counter-NBI scenario

Building on the work of Vallar et al. [12], a counter-NBI scenario was developed with on-axis plasma. Figure 1(a) illustrates the basic time traces of such a discharge. Low-current plasmas ($I_p \approx 120 \text{ kA}$) in deuterium were heated with NBI-2, leading to strong AE activity. The combination of low current and density increases the slowing-down time of fast ions, enhances radial gradients, and thereby strengthens AE drive.

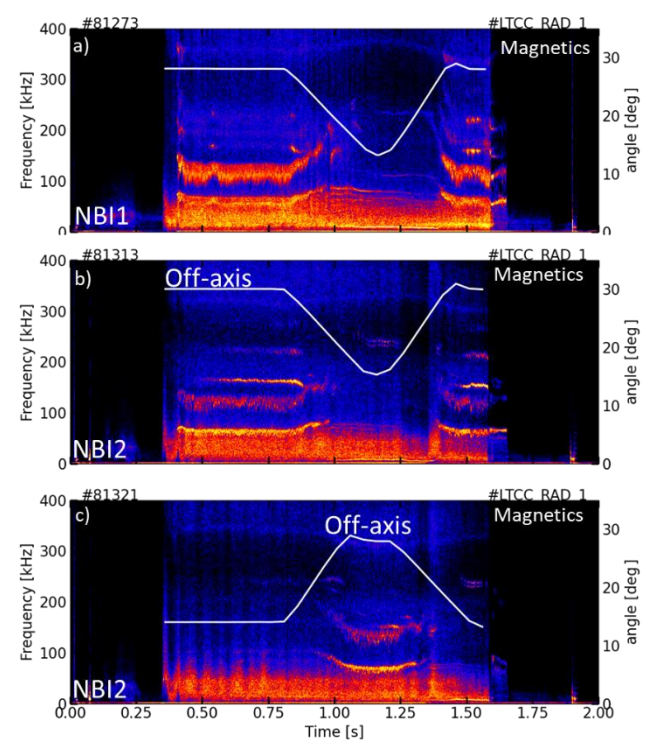


FIG 2: Spectrograms of the LTCC-radial signal for discharges with (a) NBI-1 and (b) NBI-2 counter-injection. (c) Case with ECRH deposition swept from on-axis to off-axis, in contrast to the examples shown in Fig. 1.

associated with localized heating.

Figure 1(b) presents a spectrogram from magnetic pickup coils (LTCC-radial [13]). As indicated by the white arrows, strong MHD activity is observed between 80 and 200 kHz. The lowest- and highest-frequency branches are relatively narrowband (possibly harmonics), while the central branch around 120 kHz displays a broader, chirping character. These modes appear shortly after NBI-2 is switched on. The ECRH, which is ramped up prior to NBI injection and cuts out before the end of the NBI phase, clearly modifies this activity. The lower-frequency modes persist until the beam is ramped down near 1.7 s, while other branches are suppressed.

Figure 1(c) shows the ECRH mirror angles for launchers L1 and L4, together with the TORAY-calculated deposition profile. The mirror sweep from 30° to 16° between 0.8 and 1.1 s shifts the deposition from off-axis ($\rho \approx 0.6$) towards more central values ($\rho \approx 0.25$), before returning to the original position. During this sweep, the AE frequencies shift and the mode amplitudes fade out, indicating suppression

The counter-NBI scenario is found to reliably excite AEs using either NBI-2, as shown in Fig. 1, or NBI-1, as shown in Fig. 2. Figure 2(a) presents the spectrogram of the LTCC-radial signal during NBI-1 injection. Similar to the NBI-2 case, mode activity appears during the beam-on phase. However, in this case the modes exhibit a broader-band, chirping character, suggesting that despite the lower injection energy of NBI-1 (28 keV compared to 50 keV for NBI-2), the modes are more strongly destabilized.

The robustness of AE suppression by on-axis ECRH is further demonstrated in Fig. 2(c). In this scenario the ECRH launchers were initially directed on-axis, in contrast to the off-axis configuration used previously. During the on-axis heating phase, AE activity is strongly reduced. As soon as the mirror angles are swept outward to 30°, moving the deposition off-axis, the modes reappear with significant amplitude. This provides clear evidence that localized central heating can suppress beam-driven AEs, while off-axis heating is less effective.

Mode number analysis indicates that the observed instabilities correspond to n=0 modes. In particular, the lower-frequency branch around 80 kHz exhibits features consistent with energetic particle-driven geodesic acoustic modes (EGAMs), as previously reported on TCV [14]. Although the spatial localization of these modes could not be experimentally verified, frequency analysis following the method of [15], together with available plasma profiles, suggests activity centered near mid-radius ($\rho \approx 0.5$). Ongoing MISHKA modeling aims to clarify the nature of these instabilities and to discriminate among the various n=0 Alfvénic candidates.

The predominance of n = 0 modes in counter-NBI scenarios highlights a limitation of this configuration for investigating toroidally induced AEs. To address this, a dedicated co-NBI scenario was developed with the specific goal of reliably driving toroidal Alfvén eigenmodes (TAEs).

2.1.2. Co-NBI scenario

The main difficulty in destabilizing TAEs lies in achieving sufficient fast-ion drive to overcome the stabilizing influence of shear and the closing of continuum gaps. Significant gradients in the fast-ion distribution are required, yet reduced fast-ion losses in co-current injection, compared to counter-injection, have made this challenging. In earlier studies, off-axis NBI was applied by shifting the plasma axis vertically by about 10 cm, thereby enhancing radial fast-ion gradients. The drawback of this approach, however, was the loss of diagnostic coverage, particularly from the charge-exchange system, which provides ion temperature and velocity profiles.

In the recent campaign, co-NBI was applied to plasmas centered on machine axis, enabling excellent diagnostic coverage. Figure 3 illustrates two discharges heated with NBI-1 in co-injection. The plasma current and toroidal magnetic field were the same as in the counter-NBI scenarios. In both cases, substantial ECRH heating (≈1.3 MW) was applied off-axis. Power scans established that a minimum of 900 kW of injected NBI power is required to destabilize AEs. As shown in Fig. 3(a), 700 kW produces only weak n = -3 and -4modes. When the power is increased to 950 kW in discharge

#87646 [Fig. 3(b)], the mode amplitudes grow substantially, and a clear n=-1 mode branch appears.

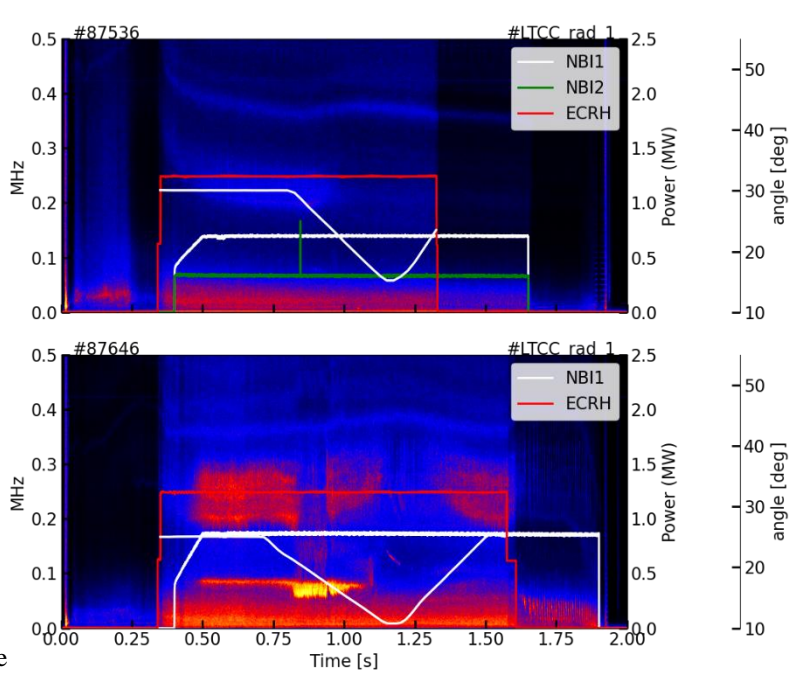


FIG 3: Spectrograms of LTCC-radial data for discharges (a) #87536 with 700 kW of co-NBI-1 injection and (b) #87646 with 950 kW of co-NBI-1. Strong MHD modes appear in the higher-power case.

Mode number analysis identifies the low-frequency branch around 100 kHz as n=-1, while the two higher-frequency branches correspond to n=-3 and -4. Interestingly, no n=-2 activity is observed, although in discharges with co-NBI-2 both n=1 and n=2 modes are detected. As in the counter-NBI scenario, these instabilities appear during phases of off-axis ECRH heating. When the deposition is moved inward, the modes sweep upward in frequency and gradually fade, before reappearing once the deposition is returned off-axis within the same discharge.

Development of high-power co-NBI scenarios is ongoing. At present, the injected power is limited at low density due to shine-through, which heats the beam dump tiles and leads to interlocks. This limitation is exacerbated by wall loading from the large ECRH power and by restrictions on accessible plasma configurations.

2.2. AE in NT vs PT plasmas

In addition to active control through actuators, plasma shaping provides a complementary means to influence AE stability. Owing to the flexibility of TCV, mirrored negative triangularity (NT) and positive triangularity (PT) plasma shapes have been studied under otherwise identical conditions. Previous experiments indicated that NT plasmas exhibit reduced AE drive compared to PT plasmas [6,7]. At TCV, MHD-quiescent discharges with comparable confinement properties were obtained in both NT and PT, with slightly higher fast-ion density typically measured in NT plasmas.

A scenario with reliable AE excitation in NT was developed using counter-NBI. Figure 4 compares discharges #82859 (NT, $\delta \approx$ -0.3) and #82861 (PT, $\delta \approx$ +0.3). Both plasmas were heated with the same toroidal magnetic field, plasma current, and counter-NBI injection. Density and temperature profiles were reasonably well matched, with NT showing a slightly higher density, thus providing a good basis for assessing the impact of triangularity on AE activity.

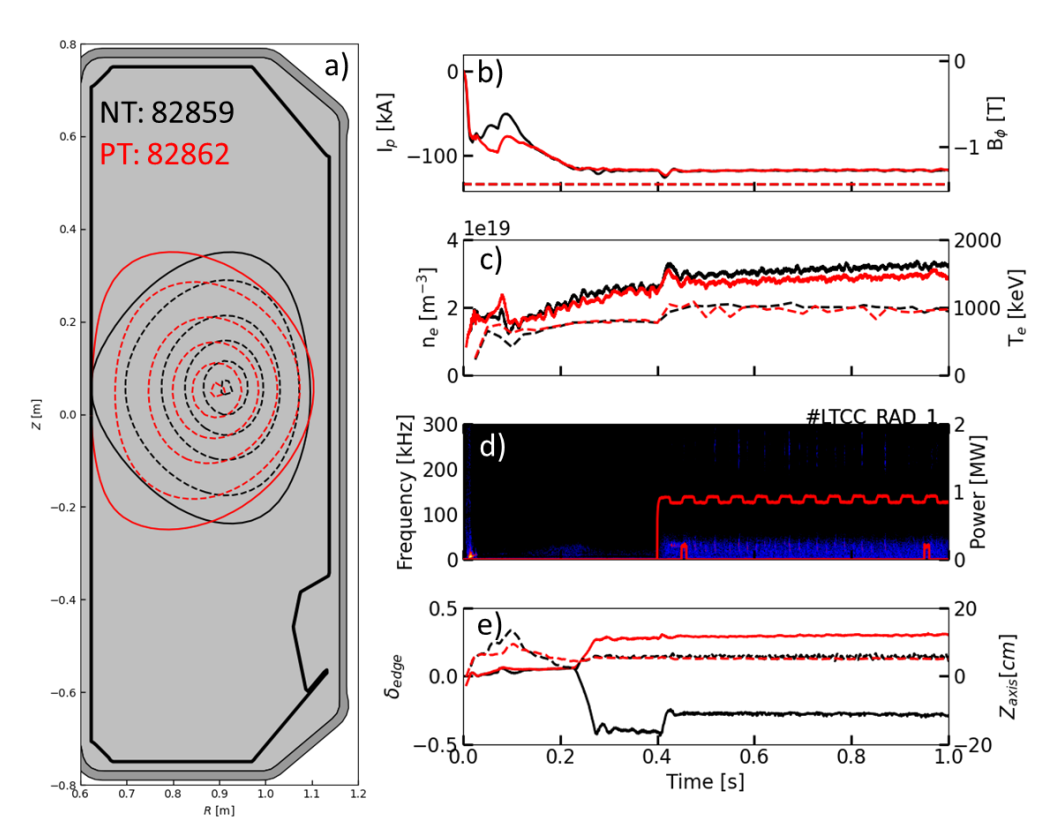


FIG 4: Comparison of (a) negative triangularity discharge #82859 ($\delta \approx -0.3$) and (b) positive triangularity discharge #82861 ($\delta \approx +0.3$), both heated with counter-NBI under otherwise similar conditions.

Figures 5 (a, c) show spectrograms of the LTCC signal, while Figs. 5(b, d) present corresponding spectrograms from the fast-ion loss detector (FILD). In both discharges, significant MHD activity is observed, but the mode amplitudes in PT are clearly larger (note that the same color scale is used). In NT plasmas, a strong mode is consistently found near 80 kHz, possibly an EGAM-type mode, whereas in PT plasmas this mode tends to appear with smaller amplitude. When off-axis ECRH was deposited near $\rho\approx 0.5$ with power increased to 1.5 MW (at t ≈ 0.8 s), the 80 kHz mode was suppressed and replaced by a narrow-band n=1 mode, likely a TAE. This n = 1 mode exhibited a larger amplitude in PT than in NT.

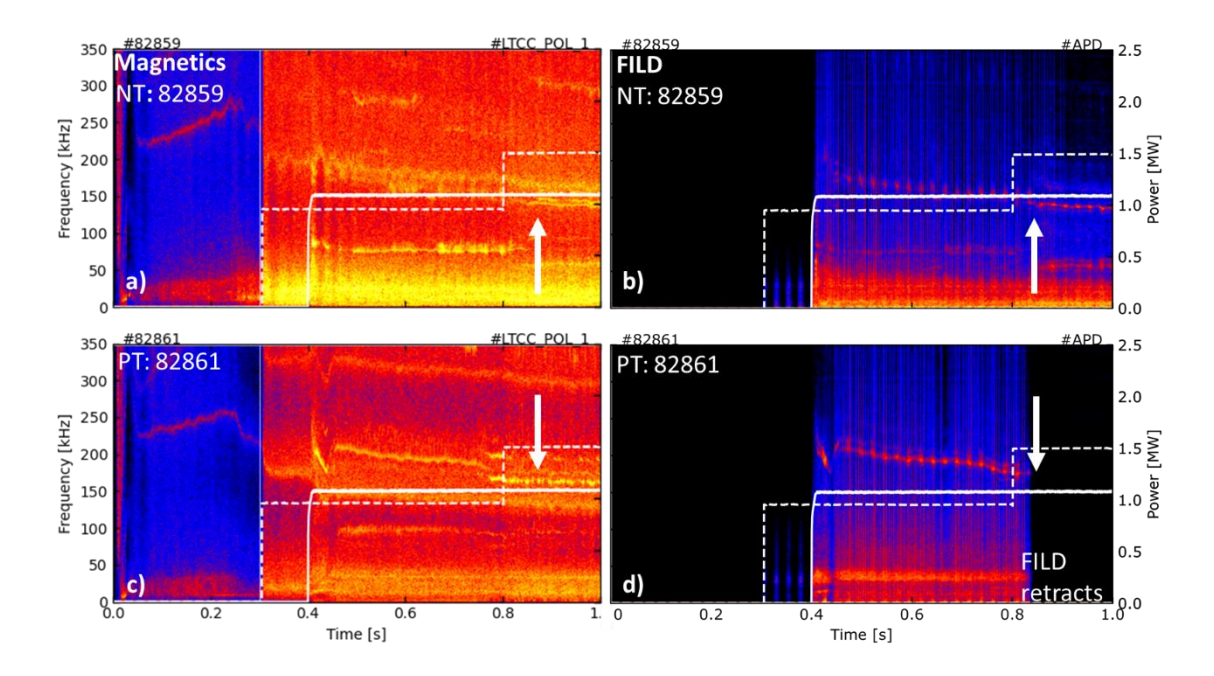


FIG 5: (a, c) LTCC spectrograms and (b, d) FILD spectrograms for the NT discharge #82859 (top) and PT discharge #82861 (bottom). Both plasmas exhibit significant AE activity, with mode amplitudes and fast-ion losses larger in PT than in NT. ECRH applied near $\rho \approx 0.5$ at $t \approx 0.8$ s suppresses the dominant 80 kHz mode and leads to the appearance of a narrow-band n=1 mode in both discharges.

The FILD measurements confirm stronger fast-ion losses in PT compared to NT discharges. However, in the PT case the detector retracted after about 0.8 s due to overheating, preventing a direct comparison during the n=1 mode phase. Ongoing experiments aim to extend these studies, though they are complicated by large wall heat fluxes in the limited plasma configurations, which often trigger FILD interlocks.

3. DISCUSSION

The experiments presented demonstrate the versatility of TCV for exploring energetic particle mode physics and control. In counter-NBI scenarios, reliable excitation of AEs was achieved, but the observed activity was dominated by n=0 modes, consistent with EGAMs. These modes were found to be strongly influenced by localized heating. Central ECRH deposition suppressed their activity, while off-axis heating allowed them to reappear. This highlights the sensitivity of n=0 modes to changes in local temperature and density profiles and shows that even in low-current plasmas ECRH can be an effective actuator for energetic particle instabilities.

In co-NBI scenarios, TAEs were successfully destabilized near the magnetic axis, overcoming the limitations of earlier off-axis approaches that restricted diagnostic access. Power scans established a clear threshold near 900 kW of injected NBI power, above which robust n=-1, -3 and -4 modes were observed. These instabilities were again sensitive to the radial location of ECRH. Off-axis heating favored mode excitation, while inward deposition led to suppression. This demonstrates the dual role of ECRH as both a destabilizing and stabilizing actuator, depending on deposition geometry.

Shaping studies further revealed that triangularity plays an important role in AE behavior. NT plasmas consistently exhibited reduced AE amplitudes compared to mirrored PT configurations under otherwise similar conditions. While both geometries supported similar types of instabilities, the dominant modes in PT plasmas were larger in amplitude and associated with stronger fast-ion losses, as measured by FILD. These results support the interpretation that NT shaping not only improves bulk confinement but also passively mitigates AE activity, offering a complementary control mechanism to active actuators such as ECRH and ECCD.

4. CONCLUSIONS AND OUTLOOK

Systematic studies on TCV have demonstrated both active and passive control of energetic particle modes. Counter-NBI scenarios provided reproducible AE excitation dominated by n=0 modes, which were shown to be suppressed by on-axis ECRH. Co-NBI scenarios enabled the reliable destabilization of TAEs near the magnetic axis, with a clear power threshold around 900 kW and strong sensitivity to ECRH deposition location. Shaping experiments confirmed that NT plasmas reduce AE amplitude and associated fast-ion losses compared to PT plasmas.

These results highlight the value of TCV as a flexible platform for energetic particle physics, combining actuator studies with shaping effects in regimes directly relevant to next-step devices. The ability of ECRH to both suppress and destabilize AEs, depending on deposition, underscores its potential as a control actuator for ITER, where localized heating and current drive will be available. The reduced AE drive in NT plasmas further suggests that shaping optimization could provide a passive pathway for improving fast-ion confinement in reactor scenarios.

Future work will include systematic ECCD scans to investigate the impact of driven current on AE stability, extended co-NBI scenarios with higher power, and refined modeling using TRANSP and ASCOT to constrain the fast-ion distribution. Continued shaping studies, combined with improved fast-ion diagnostics, will help to establish the robustness of NT as a passive AE mitigation strategy. Together, these efforts contribute directly to developing the physics basis for energetic particle control in ITER and DEMO.

ACKNOWLEDGEMENTS

This work was supported in part by the Swiss National Science Foundation. This work has been carried out within the framework of the EUROfusion Consortium, partially funded by the European Union via the Euratom Research and Training Programme (Grant Agreement No 101052200 — EUROfusion). The Swiss contribution to this work has been funded by the Swiss State Secretariat for Education, Research and Innovation (SERI). Views and opinions expressed are however those of the author(s) only and do not necessarily reflect those of the European Union, the European Commission or SERI. Neither the European Union nor the European Commission nor SERI can be held responsible for them.

REFERENCES

- [1] A. FASOLI et al., Physics of energetic ions. Nucl. Fusion 47 (2007) S264.
- [2] S. D PINCHES et al., Energetic ions in ITER plasmas. Phys. Plasmas 22 (2015) 021807.
- [3] M. GARCIA-MUÑOZ *et al.*, Active control of Alfvén eigenmodes in magnetically confined toroidal plasmas. *Plasma Phys. Control. Fusion* **61** (2019) 054007.
- [4] J. GONZALEZ-MARTIN *et al.*, Active Control of Alfvén Eigenmodes by Externally Applied 3D Magnetic Perturbations. *Phys. Rev. Lett.* **130** (2023) 035101.
- [5] S. E. SHARAPOV *et al.*, The effects of electron cyclotron heating and current drive on toroidal Alfvén eigenmodes in tokamak plasmas. *Plasma Phys. Control. Fusion* **60** (2018) 014026.
- [6] M. A. VAN ZEELAND *et al.*, Alfvén eigenmodes and fast ion transport in negative triangularity DIII-D plasmas. *Nucl. Fusion* **59** (2019) 086028.
- [7] P. OYOLA *et al.*, Mitigation of Alfvén eigenmodes in negative triangularity plasmas at the TCV tokamak, *Proc. 29th Int. Conf. on Fusion Energy (London, 2023), IAEA, Vienna*.B.P. DUVAL et al., Experimental research on the TCV tokamak. Nucl. Fusion 64 (2024) 112023.
- [8] A. N. KARPUSHOV *et al.*, Upgrade of the neutral beam heating system on the TCV tokamak second high energy neutral beam. *Fusion Eng. Des.* **187** (2023) 113384.
- [9] M. PODESTÀ et al., "Energetic particle studies on TCV". 18th Meeting on Energetic Particles, Seville (Spain), 2025.
- [10] M. VALLAR *et al.*, Excitation of toroidal Alfvén eigenmodes with counter-current NBI in the TCV tokamak. *Nucl. Fusion* **63** (2023) 046003.
- [11] B. GEIGER *et al.*, Observation of Alfvén Eigenmodes driven by off-axis neutral beam injection in the TCV tokamak. *Plasma Phys. Control. Fusion* **62** (2020) 095017.

IAEA-CN-316/2917

- [12] D. TESTA *et al.*, 3D, LTCC-type, high-frequency magnetic sensors for the TCV Tokamak. *Fusion Eng. Des.* **96-97** (2015) 989-992.
- [13] M. B. DREVAL *et al.*, Experimental investigation of the radial structure of energetic particle driven GAM in TCV. *Nucl. Fusion* **65** (2025) 016037
- [14] W. W. HEIDBRINK *et al.*, Stability of beta-induced Alfvén eigenmodes (BAE) in DIII-D. *Nucl. Fusion* **61** (2021) 066031